Pharm Res
DOI 10.1007/s11095-016-2084-0

RESEARCH PAPER

Intra- and Extracellular Biosynthesis and Characterization of Iron Nanoparticles from Prokaryotic Microorganisms with Anticoagulant Activity

Karina A. Crespo[1] • José L. Baronetti[1,2] • Melisa A. Quinteros[1,4] • Paulina L. Páez[3,4] • María G. Paraje[1,2]

Received: 4 October 2016 / Accepted: 8 December 2016

ABSTRACT

Background The use of microorganisms for the synthesis of nanoparticles (NPs) is relatively new in basic research and technology areas.

Purpose This work was conducted to optimized the biosynthesis of iron NPs intra- and extracellular by *Escherichia coli* or *Pseudomonas aeruginosa* and to evaluate their anticoagulant activity.

Study Design/Methods The structures and properties of the iron NPs were investigated by Ultraviolet–visible (UV-vis) spectroscopy, Zeta potential, Dynamic light scattering (DLS), Field emission scanning electron microscope (FESEM)/ Energy dispersive X-ray (EDX) and transmission electron microscopy (TEM). Anticoagulant activity was determined by conducting trials of Thrombin Time (TT), Activated Partial Prothrombin Time (APTT) and Prothrombin Time (PT).

Results UV-vis spectrum of the aqueous medium containing iron NPs showed a peak at 275 nm. The forming of iron NPs was confirmed by FESEM/ EDX, and TEM. The morphology was spherical shapes mostly with low polydispersity and the average particle diameter was 23 ± 1 nm. Iron NPs showed anticoagulant activity by the activation of extrinsic pathway.

Conclusion The eco-friendly process of biosynthesis of iron NPs employing prokaryotic microorganisms presents a good anticoagulant activity. This could be explored as promising candidates for a variety of biomedical and pharmaceutical applications.

KEY WORDS anticoagulant activity · *Escherichia coli* · iron nanoparticles · microbial biosynthesis · *Pseudomonas aeruginosa*

ABBREVIATIONS

APTT	Activated protombin time test
DLS	Dynamic light scattering
EDX	Energy dispersive X-ray
FESEM	Field emission scanning electron microscope
NPs	Nanoparticles
PT	Protombin time
SPR	Surface plasmon resonance
TEM	Transmission electron microscopy
TSB	Trypticase soy broth
TT	Thrombin time
UV-vis	Ultraviolet-visible

INTRODUCTION

Nanoparticles (NPs) are particles in the range of a nanometer scale having currently immense interest in basic research and technology areas because their unique properties and applications (1). There are different ways to synthesize them such as physical, chemical and biological methods (2–4). Although the physical and chemical methods are more popular, the use of toxic chemicals greatly limits their biomedical applications particularly in medical fields. This is why the development of reliable methods of synthesis, non-toxic and

✉ María G. Paraje
gabrielaparaje@gmail.com

[1] Instituto Multidisciplinario de Biología Vegetal (IMBIV) - Consejo Nacional de Investigaciones Científicas y Técnicas (CONICET), Buenos Aires, Argentina

[2] Cátedra de Microbiología, Facultad de Ciencias Exactas Físicas y Naturales, Universidad Nacional de Córdoba (UNC), Av. Vélez Sarsfield 299, Córdoba, Argentina

[3] Unidad de Tecnología Farmacéutica (UNITEFA) - Consejo Nacional de Investigaciones Científicas y Técnicas (CONICET), Buenos Aires, Argentina

[4] Departamento de Farmacia, Facultad de Ciencias Químicas, Universidad Nacional de Córdoba (UNC), Córdoba, Argentina

Published online: 19 December 2016

environmentally friendly is paramount to expand their biomedical applications. In addition, the use of natural products as anticoagulants have been extensively investigated, since these products presents low toxicity and side effects.

The three most common forms of iron oxides in nature are magnetite (Fe_3O_4), maghemite (γ-Fe_2O_3), and hematite (α-Fe_2O_3). During the synthesis, the simultaneity of Fe_3O_4 and γ-Fe_2O_3 can be attributed to the oxidation of magnetite to maghemite. They are made of a magnetic domain and consequently, show the superparamagnetic behavior and only retain magnetic moment in the presence of an external magnetic field. On detaching magnetic field, these NPs will immediately return to their nonmagnetic states. After the microbial synthesis, iron NPs rapidly form layers of iron oxide at their surface. These oxides are also very important in the field of scientific technology and for biomedical uses; NPs have low toxicity, unique properties, such as superparamagnetism, greater surface area, catalytic properties and easy separation methodology (5,6). In addition, for biomedical applications, are preferred the use of magnetic NPs that present superparamagnetic behavior at room temperature and are stable in a physiological environment (6,7). However, the extreme reactivity of iron makes it difficult to study and have some inconvenient. Is well reported the low-field response when are magnetizing (susceptibility) or demagnetizing (coercivity). The magnetic effects of a magnetic oxide cannot be easily accounted for, as nanoscale ferrimagnetic oxides are known to have reduced σs values as well (6).

The colloidal stability of NPs will be subject to the charge and surface chemistry, which give rise to both steric and coulombic repulsions and also depend on the size of the NPs, which should be sufficiently small so that precipitation due to gravitation forces can be avoided (7). For medical uses in protein immobilization, such as for diagnostic magnetic resonance imaging, thermal therapy, and drug delivery is crucial developed protection strategies to chemically stabilize the naked magnetic nanoparticles against degradation during or after the synthesis. These strategies comprise grafting of or coating with an inorganic layer, or coating with organic species (6–8).

One choice for achieving this objective is the use of microorganisms to NPs synthesis such as fungi, yeasts, bacteria and algae (4). Bacteria are interesting types of microorganisms that have an innate ability to reduce metal ions to their respective metal NPs. This mechanism of reduction of bacteria is due to its chemical detoxification acting as defense (9). Therefore, this type of biosynthesis is booming, the exact mechanism through which it occurs is not yet clears (10).

The microbial synthesis of NPs has emerged as a promising field of research that involves both the applied microbiology and the nanotechnology area, NPs are of great interest in a wide range of disciplines, including magnetic fluids, catalysis, biotechnology and biomedicine, magnetic resonance images, data storage and environmental remediation (7,11,12).

The present work was performed with the aim of knowing the optimal conditions of the extracellular and intracellular iron NPs synthesis by *Escherichia coli* and *Pseudomonas aeruginosa*. In addition to, it was carried out the evaluation of anticoagulant activity through the determination of the Thrombin Time (TT), Activated Protombin Time Test (APTT) and Protombin Time (PT).

MATERIAL AND METHODS

The reagents of analytic grade ($FeSO_4 \cdot 6H_2O$, $FeCl_3 \cdot 6H_2O$, iron citrate – Cicarelli, Argentina) were used as raw materials. Trypticase Soy Broth (TSB - Britania, Argentina). Coagulometric reagent/assay: citrate, TT, APTT and PT (Wiener Lab, Argentina).

Strains and Biosynthesis Culture Conditions

E. coli ATCC 25922 and *P. aeruginosa* ATCC 27853 were grown by inoculating a single colony from the stock culture into conical-flask containing 100 mL in TSB under agitation at 200 rpm at 37°C for 18 h. Prior to all the assays, *E. coli* or *P. aeruginosa* was grown onto Trypticase Soy agar to purity and viability control. For long-term storage, both strains were kept with 15% glycerol (v/v) at −80°C freezer (13).

For intracellular biosynthesis, 15 mL of bacteria culture was incubated with different metal solutions ($FeSO_4$, $FeCl_3$ or iron citrate). The solution was then sonicated at 80 W for 30 min and after centrifuged at 8500 rpm for 5 min.

For extracellular biosynthesis, the culture was centrifuged and the supernatant was mixed with salt ($FeSO_4$, $FeCl_3$, iron citrate) solutions avoiding the sonication process. Salt concentrations (1 and 10 mM), pH (6.5 and 9), incubation time (24, 48 and 72 h), temperature range (37 and 50°C) and relationship between the amount microbial supernatant, were tested.

NPs generation by Ultraviolet-visible (UV-vis) spectroscopy (Shimadzu 160A spectrophotometer, Japan) between 200-800 nm, in which the surface plasmon resonance (SPR) was monitored (14–16).

Characterization of the Iron NPs

Particle size and Zeta-potential iron NPs were determined by Dynamic light scattering (DLS) (Beckman Coulter, Delsa Nano C instrument, USA) (14, 15).

Field emission scanning electron microscope (FESEM)/Energy dispersive X-ray (EDX) (Carl Zeiss Sigma VP, United States) operating at 12 kV was used to acquire scanning electron microscope images.

The morphology of the resulting biosynthetic NPs were analyzed using a Transmission electron microscopy (TEM)

at 120,000 magnifications (Jeol, JEM1200 EXII, USA) and the photographs were taken at 80 kV (14,16,17).

Anticoagulation Activity of Iron NPs

Human plasma was obtained from citrated blood of healthy individuals after University Human Ethics Committee protocol (UNC) approval and with the patient informed consent.

TT is supported on the measurement of the time required for clot plasma decalcified at 37°C with an activated thrombin solution. For TT, 0.2 mL of human plasma was incubated at 37°C, together with 0.06 mL of iron NPs (2.4 mg/mL) for 300 sec. When 0.2 mL of reagent (bovine thrombin) it was added, resulted in the formation of the clot according to the manufacturer instructions and clotting times were determined in seconds (18,19).

In APTT was used an excess of cefalina, activator, calcium and it wasevaluated the time that stayed on coagulating the plasma decalcified. 0.01 mL of human plasma, 0.10 mL of the APTT reagent and 0.06 mL of iron NPs (2.4 mg/mL) were incubated for 300 sec at 37°C. Then, 0.1 mL of 0.025 mM $CaCl_2$ was aggregated and the time of formation of the clot was evaluated. Clotting times were determined in seconds (18,20).

PT is a test which determines the delay time to coagulate plasma decalcified with an excess of tissue thromboplastin and calcium at 37°C. Through this process are not detected deficiencies of factors of the track intrinsic (VIII, IX, XI and XII). It was added 0.1 mL of human plasma with 0.1 mL of iron NPs (2.4 mg/mL) and it was incubated for 60 sec at 37°C. Clot generation started by the addition of 0.2 mL of an initiator of the extrinsic pathway (the thromboplastin of brain of rabbit) and was determined in seconds (18,21).

Statistical Analysis

All assays were performed in triplicate and in three independent experiments, and the averages and standard deviations were calculated for all of them. Numerical data were presented as means ± standard deviation. Data were analyzed by using ANOVA followed by the Student-Newman-Keuls test for multiple comparisons, $^{*}p < 0.005$ were considered significant for comparisons with control.

RESULTS

Biosynthesis of Iron NPs

Iron NPs were synthesized from Fe^{2+} by treating the microbial supernatant of *E. coli* or *P. aeruginosa* and the different conditions were detailed and summarized in Tables I and II, respectively. For *E. coli*, iron NPs were formed extra- and intracellularly at 1 mM (entry 1, 3, 5, 6 and 7, 9, 10, respectively) (Table I). For *P. aeruginosa*, iron NPs were obtained only extracellularly at 1 mM (entry 1, 3, 5-7, 9, 10 – Table II). Nevertheless this production was not observed for 10 mM with both microorganisms (entry 2, 8 in Table I and 2, 8, 12 in Table II).

Iron NPs are formed extracellularly with different metallic salts ($FeSO_4$, iron citrate) at pH 6.5 in *E. coli* (entry 1 and 5, Table I) or *P. aeruginosa* (entry 1 and 9, Table II). While the SPR band was not visualized in the UV-vis spectrum with $FeCl_3$ in *E. coli* (entry 4, Table I). By increasing the pH to 9, iron NPs were generated from iron citrate and $FeSO_4$ by *E. coli* (entry 3 and 6, Table I), and iron citrate in *P. aeruginosa* (entry 10, Table II). However, they were not detected extracellularly to pH 9 in *P. aeruginosa* with $FeSO_4$ (entry 4, Table II).

When the amount of metal salt was increased it only produced a band of greater intensity in the extracellular biosynthesis with *P. aeruginosa* and $FeSO_4$ (entry 1 and 3, Table II).

Biosynthesis times were ranged from 24 to 72 h and not significant differences were observed in the SPR peak by *P. aeruginosa* (entry 5, 6 and 7, Table II) and *E. coli* (data no shown).

Table I Different Conditions of Iron NPs Biosynthesized from *E. coli* ATCC 25922 at 37°C

Entry	Metallic concentration	Biosynthesis	Ratio microor./ metallic salt	pH / time	SPR (Abs)
1	1mM $FeSO_4$	Extracellular	10	pH 6.5- 48h	0.3
2	10mM $FeSO_4$	Extracellular	10	pH 6.5- 48h	———
3	1mM $FeSO_4$	Extracellular	10	pH 9 - 48h	0.125
4	1mM $FeCl_3$	Extracelular	10	pH 6.5- 48h	———
5	1mM iron citrate	Extracelular	10	pH 6.5- 48h	0.10
6	1mM iron citrate	Extracelular	10	pH 9 - 48h	0.075
7	1mM $FeSO_4$	Intracellular	10	pH 6.5- 48h	0.175
8	10mM $FeSO_4$	Intracellular	10	pH 6.5- 48h	———
9	1mM $FeCl_3$	Intracelular	1	pH 6.5- 48h	0.08
10	1mM $FeSO_4$	Intracellular	3	pH 6.5- 48h	0.3

Table II Different Conditions of Iron NPs Biosynthesized from *P. aeruginosa* ATCC 27853 at 37°C

Entry	Metallic Concentration	Biosynthesis	Ratio microor. / metallic salt	pH / time	SPR (Abs)
1	1mM $FeSO_4$	Extracellular	10	pH 6.5, 48h	0.20
2	10mM $FeSO_4$	Extracellular	10	pH 6.5, 48h	———
3	1mM $FeSO_4$	Extracellular	3	pH 6.5, 48h	0.7
4	1mM $FeSO_4$	Extracellular	10	pH 9 - 48h	———
5	1mM $FeCl_3$	Extracelular	10	pH 6.5- 24h	0.20
6	1mM $FeCl_3$	Extracelular	10	pH 6.5, 48h	0.25
7	1mM $FeCl_3$	Extracelular	10	pH 6.5 - 72h	0.25
8	10mM $FeCl_3$	Extracelular	10	pH 6.5, 48h	———
9	1mM iron citrate	Extracelular	10	pH 6.5, 48h	0.30
10	1mM iron citrate	Extracelular	10	pH 9, 48h	0.175
11	1mM $FeSO_4$	Intracellular	10	pH 6.5, 48h	———
12	10mM $FeSO_4$	Intracellular	10	pH 6.5, 48h	———

In summary, the optimal conditions for *E. coli* or *P. aeruginosa* were extracellular biosynthesis using 1 mM $FeSO_4$ at pH 6.5 for 48 h and 37°C.

However, iron NPs extracellular biosynthesis by *E. coli* was selected for characterization, because the supernatant of *P. aeruginosa* releases higher amount of extracellular substance than *E. coli* at supernatant that make dirty the culture medium.

Characterization of Iron NPs

The NPs were characterized by UV-vis spectroscopy. The soft SPR peak was centered at approximately 275 nm (Fig. 1a). The size of iron NPs was measured by DLS technique which analyzes particle size distribution in the solution phase based on the random changes in the intensity of their scattered light. The histogram shows that particle size for iron NPs was 23 ± 1 nm (Fig. 1b). The density of electric charge, also known as zeta potential, on the surface of a particle colloidal is an essential factor in determining the stability of this system. With increased density of electric charge, the particles acquire forces repulsive more intense that prevents contact between them. Usually, the majority of colloidal particles have positive charges or negative in its surface. The surface charge of iron NPs biosynthesized in this work showed a value of -10.05 mV (Fig. 1c).

The analysis by EDX of iron NPs confirmed the presence of elemental iron signal. In the spectra of EDX was observed a peak of oxygen which suggests that the NPs biosynthesized presented an oxide layer (Fig. 2). The inset showed, as expected at iron NPs, the peaks between 0.6 to 0.8, 6.3 and 6.8 keV are related to the binding energies of Fe. The spectrum contained three peaks, which were assigned to Fe, O and C. The EDX analysis suggest that Fe, O and C (H could not be measured) are the main constituents in the magnetic NPs. The distribution of iron NPs were further investigated by FESEM. The Fig. 3a revealed the presence of spherical iron NPs (arrows), but is not the best methodology for size determination. Furthermore, the iron NPs biosynthesized was examined by TEM at 120,000 magnifications. As shown in Fig. 3b, the sizes of iron NPs biosynthesized intracellular by *E. coli* shown low polydispersity, spherical forms and the average size of the particles was 18 ± 2 nm.

Anticoagulant Activity

The iron NPs solution (2.4 mg/mL) was incubated with human plasma and assayed for coagulation time, compared to controls for each assay (Fig. 4). To evaluate if the iron NPs would generate the clots by them, NPs were incubated in absence of other opening reagents and was not observed clots. TT is an indicator of the functionality of the final common pathway of coagulation. TT showed that the time (seconds) of formation of the clot was greater (22.3 ± 0.9) than the control (18.4 ± 0.4) ($^{*}p < 0.005$).

The determination of APTT verified the inhibition of track intrinsic coagulation with iron NPs, indicated by the prolongation of the times of coagulation in this test. The APTT measurements were 34.6 ± 1.1 seconds for iron NPs compared to control level (27.3 ± 1.1) ($^{*}p < 0.005$). No significant difference was observed on coagulation with iron NPs solution (16.2 ± 0.7) in the test track extrinsic.

DISCUSSION

Iron NPs are extremely reactive with oxidizing agents, specifically with respect to water and oxygen. For the complete and permanent protection from oxidizing, each NP is covered with a thin covering that has little or no impact on the magnetic property of NPs different coating materials are used for this purpose.

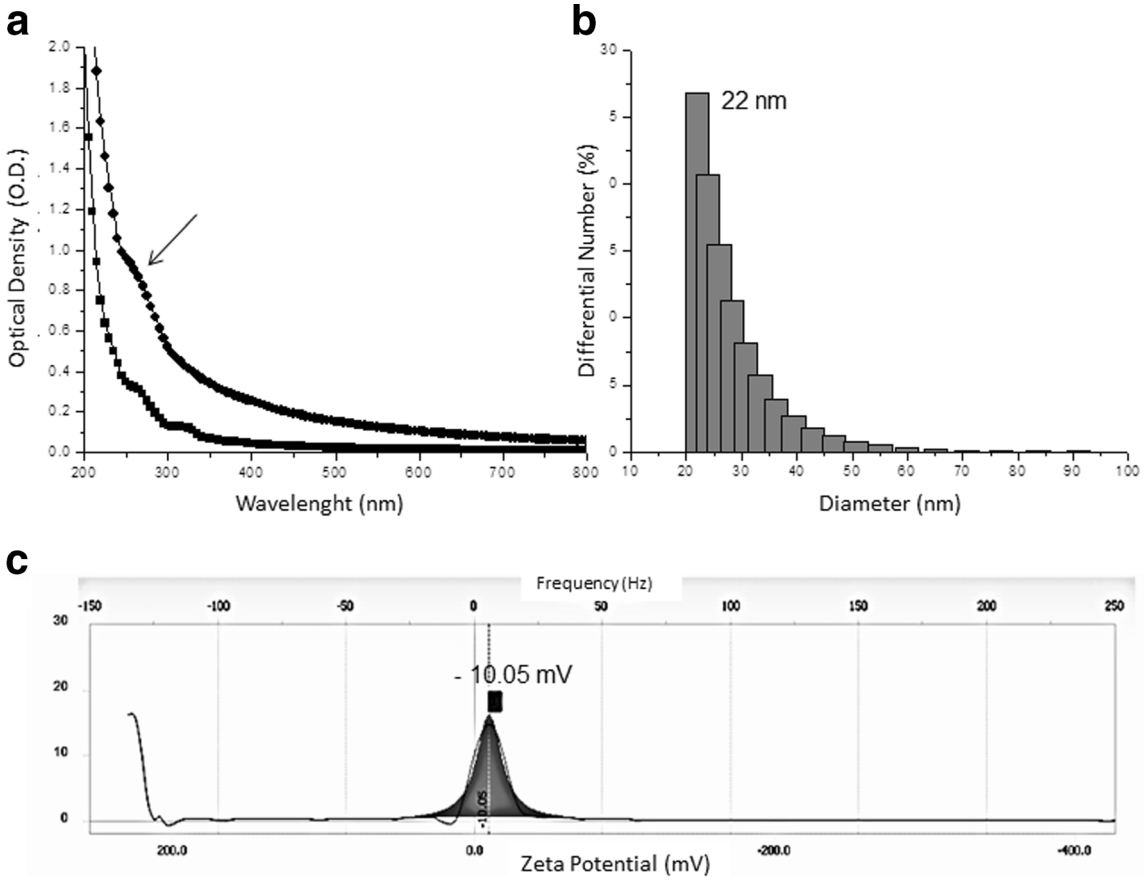

Fig. 1 Biosynthesis of iron NPs by *E. coli* ATCC 25922 monitored by UV-vis. (**a**) UV-vis absorption spectrum of control (-■-) and iron NPs (-●-). A sharp absorption peak can be observed for the iron NPs at 275 nm indicating the presence of iron (*arrows*). (**b**) Histogram obtained from DLS technique showing number distribution of biologically synthesized iron NPs. (**c**) Zeta potential analysis of iron NPs.

NPs can be synthesized by chemical, physical and biological methods. Microbial methods they have the advantage of securing ensure low cost, reproducibility, environmentally friendly, high performance and

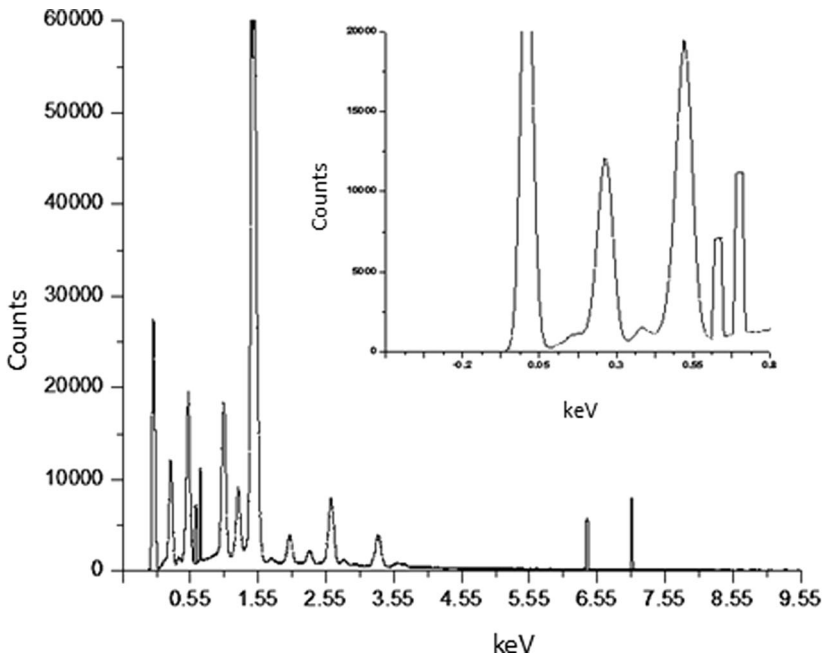

Fig. 2 Spectrum of iron NPs obtained by EDX microanalysis. *Inset*: peak of iron between 0.6 to 0.8 keV.

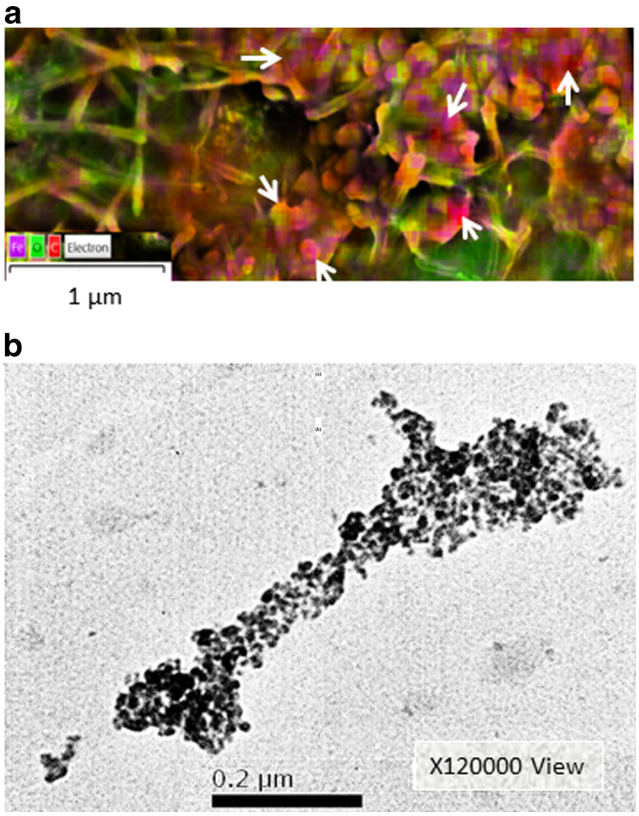

Fig. 3 (**a**) The distribution of iron NPs by FESEM. The *arrows* showed of purple color of the iron NPs (*scale bar* 1 µm). (**b**) TEM images of iron NPs synthesized by *E. coli* (120,000 magnification, *scale bar* 0.2 µm).

scalability, but require a lot of time and is laborious. This type of biosynthesis has the advantage of producing very high yields of secreted proteins, which can increase the rate of nanoparticle synthesis (6). In order to study the influence of different microbial culture condition in the NPs biosynthesis, the reaction was carried out for diverse condition as metallic concentration, different ratio between metallic salts and microorganisms and pH and time

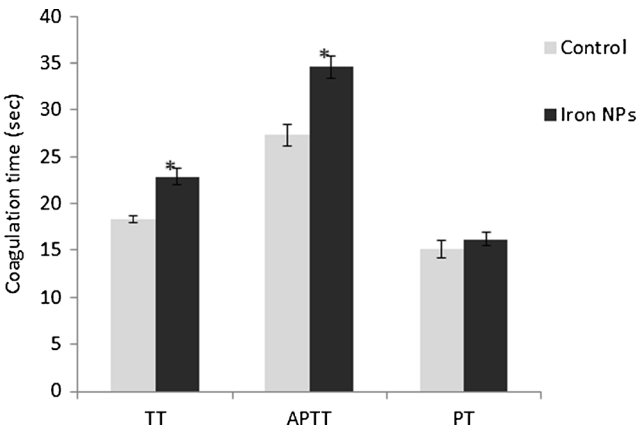

Fig. 4 *In vitro* studies of iron NPs on the blood coagulation (TT, APTT and TP) in normal human plasma. *Error bars* represent the standard deviations of the means of three independent experiments. $p < 0.005$ were considered significant for comparisons with non-treated sample (control).

condition. The preparation yield when use microorganisms in NPs biosynthesis are complex because the exact mechanism through which it occurs is not yet clears (10,11). The systems of detoxification by bacteria defense reduce metal ions to their respective metal NPs. The yield of the biosynthesis was calculated by keeping the ratio of reactive and SPR band was visualized in the UV-vis spectrum (22). The results obtained showed a higher intensity of the SPR peak corresponding to *E. coli* or *P. aeruginosa* were extracellular biosynthesis using 1 mM $FeSO_4$ at pH 6.5 for 48 h and 37°C (entry 1, Table I and entry 3, Table II) indicating that a higher yield of iron NPs compared with other conditions at the same biological reaction. NPs were obtained as a light brown color that intensifies a longer culture time until a dark brown color. The nanoparticles obtained by this method, under these conditions were stable, allowing their storage, manipulation and use in biological activity assays. In order to compare the results of the different synthesis conditions, the values of SPR (Abs) UV-vis are shown in Tables. For example, for *P. aeruginosa*, the soft SPR peak (0.20) at approximately 275 nm was observed in biosynthesis using 1 mM $FeSO_4$, however, an increase of yield of the reaction in 3.5 times when the ratio microorganism/metallic salt decrease from 10 to 3. The height relationship of the two peaks improves in favor of the disappearance of reagent and change of medium appearance.

The biosynthesis of iron NPs using *P. aeruginosa* with $FeSO_4$ only occurred extracellularly like investigations carried out by other researchers in prokaryotes organisms (23–25), while in the case of *E. coli* the formation occurred both intra and extracellularly (26). Probably, these Gram negative microorganisms are capable of reducing iron ions to iron NPs due to the presence of some enzymes present in their cellular wall structures. It has been studied that the culture supernatants of *Enterobacteriaceae* (*Klebsiella pneumoniae*, *E. coli* and *Enterobacter cloacae*) synthesizes silver NPs by means of Ag^+ reduction for Ag^0. When add piperitone the reduction of silver ions was inhibited partially, allowing to participation of nitro reductase enzymes in reducing process (9).

In this study the biosynthesis was conducted by modifying different physicochemical parameters. The use of different iron salts and ratio between metallic salts and microorganisms allowed determining which was adequate for each microorganism. Only iron NPs take place to low concentrations (1mM). The biosynthesis of iron NPs by *P. aeruginosa* occurred with all salts tested at pH 6.5. However, in *E. coli* with $FeCl_3$ were not generated NPs extracellular. To evaluate the effect of pH it was observed a decrease in the plasmon SPR due to the increase of the pH to 9. This could be caused by the inactivation or degradation of certain biological molecules responsible for the process of reduction. When we controlled time of

biosynthesis it was determined that NPs were already generated in 48 h, during the end or near the stationary phase of bacteria growth.

In addition we evaluated the effect of varying the relationship between bacterial suspension and metallic salt. If the relationship is one occurred NPs intracellularly with *E. coli*, but that various relationship three generates an increase in the SPR plasmon only for *P. aeruginosa*.

When iron solution was added to bacterial solution, the supernatant changed to a brownish color upon the completion of 48 h reaction suggested the formation of iron NPs. This color results from absorption by colloidal iron NPs in the visible region of the electromagnetic spectrum ($\lambda = 275$ nm) due to the excitation of surface plasmon vibrations. The UV spectroscopy technique has proved to be very useful for the analysis of NPs (27). Observation of the soft but broad SPR peak has been well documented for several metallic NPs, with sizes ranging from 2 to 100 nm (28). The SPR band at lower wavelengths (200-300 nm) would indicate that the colloidal dispersion is composed primarily of iron NPs spherical and small. The shape and size of the iron NPs were confirmed by DLS, FESEM/EDX and TEM. These results are consistent with those obtained by other investigators (29,30).

Under biosynthesis conditions, Fe_3O_4 NPs are not very stable and can easily be oxidized to Fe_2O_3 or dissolve in an acidic medium. Chemically, the iron oxide NPs are very active and can easily be oxidized (especially magnetite), generally resulting in the loss of dispensability and magnetism. For another hand, the pH of the growth medium is also important for *E.coli* growth rate and cell density. The optimal growth pH for *E.coli* is near neutral, but can grow reasonably well over a range of three pH units (from pH 5.5 to 9). Extreme pH beyond this range will significantly decrease the cell growth rate and may sometimes even cause cell death. *E.coli* cells can grow on a solid medium plate at pH 11, but they cannot grow in a liquid media with pH 9 or higher. In Table I, SPR (Abs) of iron NPs biosynthesized from *E. coli* was 2.4 times higher at pH 6.5 than to pH 9. Nevertheless this production was not observed for pH 9 with *P. aeruginosa*. The pH range assays during the biological synthesis of iron oxide NPs was from 5.5 to 9, when the optimal to 6.5 (31).

The impact of pH on surface charge is typically characterized by iso-electric point (IEP), the critical pH value at which the net surface charge is zero. Lin *et al.* shows the Zeta potential of the iron NPs as a function of solution pH and IEP was found to be near pH ≈ 8.3. Comparatively, IEP of iron nanoparticles is higher than that of magnetite (Fe_3O_4) (~6.8) or maghemite (γ-Fe_2O_3) (~ 6.6) (32). We results are according with other authors the Zeta potential curves of NPs Fe_2O_3 as a function of pH. The measured isoelectric point of the γ-Fe_2O_3 particles is at about pH 6.7. The Zeta potential curve for the synthesized NPs suggests a "passive surface for the uncoated iron oxide, with the Zeta potential ranging from positive values (+20 mV) at low pH values to negative values (−48 mV) at high pH. The surface change potential of γ-Fe_2O_3 particles in water could be explained by surface hydroxyl groups (FeOH). In a basic environment the surface shows negative charge potential because of formation of FeO, whereas in an acid environment the positive surface charge is except due to $FeOH_2^+$ formation (33). Values of Zeta potential between -30 to +30 mV generate stability in colloidal systems (34). However, values near zero indicate a lower stability resulting from the reduction repulsive force between the particles. In these cases, colloidal particles are the subject of flocculation (35). This value indicates that the surface of the iron NPs presented an anionic charge. The above mentioned property presents a roll like cellular signature to study the superficial interaction and cellular NPs absorption.

Anticoagulants are used in the clinic to treat or to prevent clots of blood or pulmonary embolism. When the plasma is subjected to certain nanomaterials *in vitro*, in some cases is generated an exhaustion of some clotting factor, delaying the formation of the clot (36). In this work different assays were realized to estimate if the iron biosynthesized NPs might begin or impel the process of the coagulation. It was determined that iron NPs have an anticoagulant effect on the final common pathway (TT) and in the intrinsic pathway of coagulation process (determination of APTT) and not in the extrinsic pathway (PT), indicating a potential use in medicine.

CONCLUSION

This study demonstrates the control of the microbial biosynthesis environment plays vital role in iron NPs, showed the best conditions by *E. coli* or *P. aeruginosa* extracellular biosynthesis at physiological condition. The Zeta potential, DLS, FESEM/EDX and TEM confirmed the characterizations of iron NPs. In addition, *in vitro* studies support anticoagulant activity of iron NPs by inhibition of intrinsic pathway and this opens the door for novel application in pharmacy and medicine.

ACKNOWLEDGMENTS AND DISCLOSURES

PL Páez and MG Paraje are members of the Research Career of CONICET. KA Crespo is a postdoctoral fellow of CONICET. MA Quinteros is PhD fellow of CONICET. We are also very grateful to Wiener Lab SAIC. This work

was supported by the following Grants: SECyT, FONCyT and CONICET.

COMPLIANCE WITH ETHICAL STANDARDS

Conflicts of Interest The authors declare that they have not conflict of interest.

REFERENCES

1. Larrañeta E, McCrudden MT, Courtenay AJ, Donnelly RF. Microneedles: a new frontier in nanomedicine delivery. Pharm Res. 2016;33(5):1055–73. doi:10.1007/s11095-016-1885-5.
2. Liu J, Qiao SZ, Hu QH, Lu GQ. Magnetic nanocomposites with mesoporous structures: synthesis and applications. Small. 2011;7(4):425–43.
3. Luechinger NA, Grass RN, Athanassiou EK, Stark WJ. Bottom-up fabrication of metal/metal nanocomposites from nanoparticles of immiscible metals. Chem Mater. 2010;22(1):155–60.
4. Hulkoti NI, Taranath TC. Biosynthesis of nanoparticles using microbes a review. Colloids Surf B. 2014;121:474–83.
5. Teja AS, Koh P. Synthesis, properties, and applications of magnetic iron oxide nanoparticles. Prog Crystal Growth Char Mat. 2009;55(1):22–45.
6. Ali A, Zafar H, Zia M, Ul Haq I, Phull AR, Ali JS, *et al.* Synthesis, characterization, applications, and challenges of iron oxide nanoparticles. Nanotechnol Sci Appl. 2016;9:49–67.
7. Akbarzadeh A, Samiei M, Davaran S. Magnetic nanoparticles: preparation, physical properties, and applications in biomedicine. Nanoscale Res Lett. 2012;7(1):144.
8. Hasany S, Ahmed I, Rajan J, Rehman A. Systematic review of the preparation techniques of iron oxide magnetic nanoparticles. Nanosci Nanotechnol. 2012;2(6):148–58.
9. Narayanan KB, Sakthivel N. Biological synthesis of metal nanoparticles by microbes. Adv Colloid Interface Sci. 2010;156(1-2):1–13.
10. Zhang X, Yan S, Tyagi RD, Surampalli RY. Synthesis of nanoparticles by microorganisms and their application in enhancing microbiological reaction rates. Chemosphere. 2011;82:489–94.
11. Naha PC, Lau KC, Hajfathalian M, Mian S, Chhour P, Uppuluri L, *et al.* Gold silver alloy nanoparticles (GSAN): an imaging probe for breast cancer screening with dual-energy mammography or computed tomography. Nanoscale. 2016;8(28):13740–54.
12. Gupta AK, Gupta M. Synthesis and surface engineering of iron oxide nanoparticles for biomedical applications. Biomaterials. 2005;26:3995–4021.
13. Angel Villegas N, Baronetti J, Albesa I, Etcheverría A, Becerra MC, Padola NL, *et al.* Effect of antibiotics on cellular stress generated in Shiga toxin-producing *Escherichia coli* O157:H7 and non-O157 biofilms. Toxicol In Vitro. 2015;29:1692–700.
14. Zhang J, Shin MC, Yang VC. Magnetic targeting of novel heparinized iron oxide nanoparticles evaluated in a 9L-glioma mouse model. Pharm Res. 2014;31(3):579–92.
15. Quinteros MA, Aiassa Martínez IM, Dalmasso PR, Páez PL. Silver nanoparticles: biosynthesis using an ATCC reference strain of *Pseudomonas aeruginosa* and activity as broad spectrum clinical antibacterial agents. Int J Biomater. 2016;2016:5971047. doi:10.1155/2016/5971047.
16. Quinteros MA, Cano Aristizábal V, Dalmasso PR, Paraje MG, Páez PL. Oxidative stress generation of silver nanoparticles in three bacterial genera and its relationship with the antimicrobial activity. Toxicol in Vitro. 2016;36:216–23.
17. Mohamed YM, Azzam AM, Amin BH, Safwat NA. Mycosynthesis of iron nanoparticles by *Alternaria alternata* and its antibacterial activity. Afr J Biotechnol. 2015;14(14):1234–41.
18. Wiener Lab Group. Vademecum. Reagents for Clinical Laboratory. Ed 2000. Rosario, Argentina. 2000.
19. Kern A, Várnai K, Vásárhelyi B. Thrombin generation assays and their clinical application. Orv Hetil. 2014;155(22):851–7.
20. Young DS. Effects of drugs on clinical laboratory tests. 4th ed. Washington DC: AACC Press; 2001.
21. Martínez-Gutierrez F, Thi EP, Silverman JM, de Oliveira CC, Svensson SL, Vanden Hoek A, *et al.* Antibacterial activity, inflammatory response, coagulation and cytotoxicity effects of silver nanoparticles. Nanomedicine. 2012;8:328–36.
22. Lassenberger A, Bixner O, Gruenewald T, Lichtenegger H, Zirbs R, Reimhult E. Evaluation of high-yield purification methods on monodisperse PEG-grafted iron oxide nanoparticles.
23. Bharde A, Wani A, Shouche Y, Joy PA, Prasad BLV, Sastry M. Bacterial synthesis of nanocrystalline magnetite. J Am Chem Soc. 2005;127:9326–7.
24. Lee JH, Roh Y, Hur HG. Microbial production and characterization of superparamagnetic magnetite nanoparticles by *Shewanella* sp. HN-41. J Microbiol Biotechnol. 2008;18:1572–7.
25. Roh Y, Jang HD, Suh Y. Microbial synthesis of magnetite and Mn substituted magnetite nanoparticles: influence of bacteria and incubation temperature. J Nanosci Nanotechnol. 2007;7:3938–43.
26. Quester K, Avalos-Borja M, Castro-Longoria E. Biosynthesis and microscopic study of metallic nanoparticles. Micron. 2013;54–55:1–27.
27. Gonzalo J, Serna R, Sol J, Babonneau D, Afonso C. Morphological and interaction effects on the surface plasmon resonance of metal Nanoparticles. J Phys Condens Matter. 2003;15(42):3001–2.
28. Srivastava SK, Constanti M. Room temperature biogenic synthesis of multiple nanoparticles (Ag, Pd, Fe, Rh, Ni, Ru, Pt, Co, and Li) by *Pseudomonas aeruginosa* SM1. J Nanopart Res. 2012;14:1–10.
29. Bharde A, Rautray D, Sarkar I, Seikh M, Sanyal M, Ahmad A, *et al.* Fungus mediated synthesis of magnetite nanoparticles. Small. 2006;2:135–41.
30. Lin SY, Wu SH, Chen CH. A simple strategy for prompt visual sensing by gold nanoparticles: general applications of interparticle hydrogen bonds. Angew Chem Int Ed. 2006;45(30):4948–51.
31. Mahdavi M, Ahmad MB, Haron MJ, Namvar F, Nadi B, Rahman MZ, Amin J. Synthesis, surface modification and characterization of biocompatible magnetic iron oxide nanoparticles for biomedical applications. Molecules. 2013; 27,18(7):7533–48.
32. Lin J, Weng X, Dharmarajan R, Chen Z. Characterization and reactivity of iron based nanoparticles synthesized by tea extracts under various atmospheres. Chemosphere. 2016;25(169):413–7.
33. Bini R, Marques RFC, Santos FJ, Chaker JA, Jafelicci Jr M. Synthesis and functionalization of magnetite nanoparticles with different amino-functional alkoxysilanes. J Magn Magn Mater. 2012;324(4):534–9.
34. Wang N, Hsu C, Zhu L, Tseng S, Hsu JP. Influence of metal oxide nanoparticles concentration on their zeta potential. J Colloid Interface Sci. 2013;407:22–8.
35. Shrivastava S, Bera T, Sunil Singh K, Singh G, Ramachandrarao P, Dash D. Characterization of antiplatelet properties of silver nanoparticles. ACS Nano. 2009;3:1357–64.
36. Mahdavi M, Namvar F, Ahmad MB, Mohamad R. Green biosynthesis and characterization of magnetic iron oxide (Fe_3O_4) nanoparticles using seaweed (*Sargassum muticum*) aqueous extract. Molecules. 2013;18(5):5954–64.